



Drawdown of floating solids in stirred tanks: Scale-up study using CFD modeling

Yogesh Waghmare^{a,*}, Rick Falk^a, Lisa Graham^a, Venkat Koganti^b

^a Bend Research Inc., 64550 Research Rd., Bend, OR 97701, United States

^b Pfizer Inc., Groton, CT, United States

ARTICLE INFO

Article history:

Received 4 November 2010

Received in revised form 27 April 2011

Accepted 14 May 2011

Available online 20 May 2011

Keywords:

Process development

Scale up

Modeling

Simulation

CFD

ABSTRACT

This work shows development of a scale up correlation using computational fluid dynamic (CFD) simulations for floating solids drawdown operation in stirred tanks. Discrete phase modeling (DPM) simulations were used in conjunction with the lab scale experimental measurements to develop a semi-empirical correlation for the prediction of rate of drawdown of floating solid particles. The rate was correlated to average liquid velocity at the free liquid surface. Since, this correlation is based on a fundamental hydrodynamic parameter, velocity, rather than an operating parameters such as the impeller speed, it can be used for a variety of impeller types and tank geometries. The correlation was developed based on the data obtained from the 2 L tank using four different tank designs and was validated against the data obtained from the 10 L scale tank. The correlation was further extended to the pilot and the commercial scale tanks ranging from 40 L to 4000 L scale based solely on the CFD model.

© 2011 Elsevier B.V. All rights reserved.

1. Introduction

Drawdown of floating solids is a commonly encountered process operation in the chemical process industry. Lack of a systematic methodology to scale-up mixing applications involving solids drawdown increases scale-up time and thus increasing production costs. In this work we propose a scale-up principle that can address this existing gap in our scale-up understanding of solids drawdown. Three different phenomena may cause solids to float:

- (1) Low true density – particles float because of the buoyancy force.
- (2) Low bulk density of powders – fine particulates have tendency to agglomerate and trap air resulting in the low bulk density.
- (3) Poor wettability and surface tension effects cause the surface tension force to be greater than the gravitation force.

The available data in the literature is primarily focused on low true density particles. Investigation related to the rest of the two phenomena is nonexistent because of its complexity and specificity to the solid phase material used.

Fate of a particle (whether it will float or sink) placed on free liquid surface is decided by the force balance on the particle. Fig. 1 (Khazam and Kresta, 2008) illustrates the different forces acting on a particle. Motion of the liquid phase set up by the stirrer rotations induces turbulent force and drag force on the particle. At a sufficiently high stirrer speed the downward forces overcome

the buoyancy and the surface tension forces causing drawdown of particle into the bulk liquid phase.

Khazam and Kresta (2008) identified three mechanisms of solids drawdown in stirred tanks. (1) Formation of stable single vortex (with no baffles or single baffle system) causes downward axial velocities at the surface responsible for drawdown. (2) Turbulent fluctuations form meso scale eddies/vortices on the surface which intermittently pull particles in the liquid. (3) Mean drag produced by the liquid circulation loops draw particles into the liquid where the downward axial velocities are greater than the particle slip velocity.

Drawdown performance of a stirred tank is generally characterized in terms of N_{jd} , just drawdown stirrer speed. Just drawdown speed refers to the minimum stirrer speed at which particles spend less than 2–5 s at the surface. Many investigators have reported measurement of N_{jd} using different types of tank geometries with varying impeller types, submergence, number of baffles, baffle configurations and various impeller to tank diameter ratios (Kuzmanic and Ljubic, 2001; Bakker and Frijlink, 1989; Özcan-Taşkın and Wei, 2003). Effects of the physical properties of liquids and solids as well as effects of solids loading have also been studied (Joosten et al., 1977; Khazam and Kresta, 2009). The only attempt to develop an empirical correlation to predict just drawdown speed as a function of the tank geometry and the physical properties of liquid and solids was by Joosten et al. (1977) who proposed a correlation for calculating Froude number at just drawdown speed as:

$$N_{Fr} = \frac{N_{jd}^2 D}{g} = k_1 \left(\frac{D}{T} \right)^{-3.65} \left(\frac{\rho_l - \rho_s}{\rho_l} \right)^{0.42} \quad (1)$$

* Corresponding author. Tel.: +1 5086611983.

E-mail address: ywaghmare@gmail.com (Y. Waghmare).

Nomenclature

C	impeller clearance from tank bottom (m)
D	impeller diameter (m)
g	gravitational constant (m/s^2)
H	tank height (m)
k	constant of proportionality in Eq. (4) (dimensionless)
k_1	constant of proportionality in Eq. (1) (dimensionless)
N	stirrer speed (rps)
N_{Fr}	Froude number (dimensionless)
N_{jd}	stirrer speed at just drawdown (rps)
T	tank diameter (m)
W	baffle width (m)
Z	liquid height (m)
ρ_l	density of liquid (kg/m^3)
ρ_s	density of solid (kg/m^3)

where, the proportionality constant k_1 depends on the type of impeller. N_{Fr} is Froude number, N is the stirrer speed in rps, D is the impeller diameter in m, g is the gravitational constant, T is the tank diameter in m, ρ_l is the liquid density and ρ_s is the solid density in kg/m^3 .

Based on the measurement of just drawdown speed, different researches have recommended different optimal tank designs resulting in lowest power requirement for solids drawdown and uniform distribution of particles throughout the liquid phase. General description of different types of impellers and how it affects mixing in stirred tanks is given in details by Paul et al. (2004). Most researchers found down pumping 45° pitched blade turbine (PBT) with partial baffle to be the most effective geometry but the configuration of partial baffles was different for each researcher. Joosten et al. (1977) used single baffle, Hemrajani et al. (1988) used four baffles of width $1/50$ tank diameter and Siddiqui (1993) recommended three partially immersed baffles 90° apart. Edwards and Ellis (1984) found 3 bladed marine propeller without any baffles to be the most energy efficient design. Ozcan-Taskin and McGrath (2001) suggested use of axial or mixed flow impeller mounted close

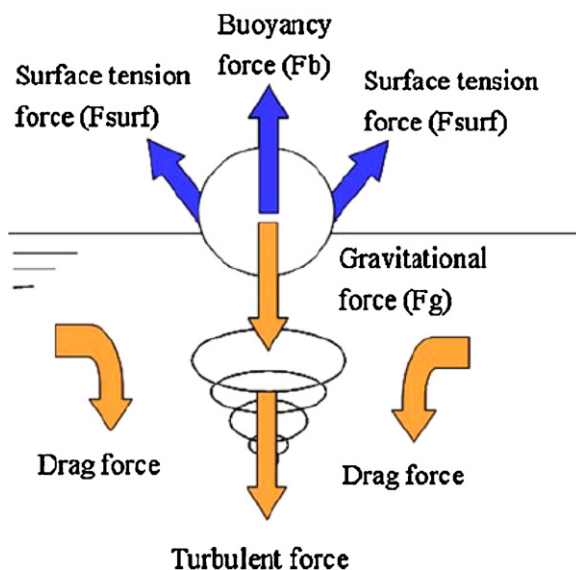


Fig. 1. Force balance around floating particle on liquid surface. Source: Khazam and Kresta, 2008.

to the tank bottom with fully baffled vessel as an optimal design. Recent study by Khazam and Kresta (2009) recommended use of four surface baffles with either up-pumping or down-pumping PBT. Özcan-Taskin (2006) studied the effect of the scale on drawdown performance. Author found power per unit volume to be a satisfactory criterion for the scale up of tanks with up-pumping PBT impeller but down-pumping impeller failed to comply with any traditional scale up criteria.

CFD modeling techniques have been routinely used in the past for modeling mixing in stirred tank vessels. Numbers of studies have investigated flow patterns and mixing in single phase stirred tank systems (Bakker and Van den Akker, 1994; Sahu et al., 1999; Kresta and Wood, 1991). More complex models have been deployed to simulate multiphase systems such as gas–liquid (Khopkar et al., 2005; Kerdouss et al., 2008), solid–liquid (Montante et al., 2001; Ljungqvist and Rasmuson, 2001) and gas–liquid–solid (Murthy et al., 2007) system. In case of solid–liquid systems, for solids heavier than liquid, CFD models have been developed to predict the just suspension speed (Derksen, 2003) and solids distribution in stirred tanks (Micale et al., 2004; Srinivasa and Jayanti, 2007). To authors knowledge no study in the past reported use of CFD for prediction of drawdown performance of floating solids. All the efforts listed in the previous paragraph were based on purely experimental measurements.

Although measurement of N_{jd} has been a standard for the drawdown performance, but the definition of N_{jd} is not standardized. Ellis et al. (1988) proposed the use of photocell to quantitatively measure the drawdown performance. The quantitative characterization was achieved by measuring the number of particles present on the surface as a function of rpm. Authors found that there were always finite number of particles present on the surface and there is no obvious minimum impeller speed that corresponds to total drawdown.

The work presented here is different than the previous literature in mainly the following three categories:

- Literature till date deals with standard tank geometries consisting of straight, centered shaft, standard impellers such as PBT, FBT. The work presented here explores solids drawdown phenomenon in non-standard tank geometries which include tilted shaft, non-standard impellers as well as multiple impellers. These non-standard tank geometries are frequently encountered in the pharmaceutical industry because of its ease of cleaning and ability to fabricate with glass material.
- Majority of the literature investigations were performed using spherical beads made up of lighter true density solids as a model compound as opposed to the powder of low bulk density solids used in this study. It should be noted that the true density of solid used for the current investigation was higher than the liquid. The floating action was caused by the entrapped air between the particles resulting in lower bulk density. Surface tension also plays a role in keeping the powder particles afloat.
- For the current study, the absolute value of drawdown rate of solids was used as a measure of performance instead of using the just drawdown speed (Kuzmanic and Ljubic, 2001; Bakker and Frijlink, 1989; Özcan-Taşkin and Wei, 2003). There is no true just drawdown speed for powders because particles once incorporated in liquid do not float back on the surface. The particles have the true density higher than the liquid phase hence the particles sink in the liquid once wet.

The early sections of this paper focus on the 2 L and the commercial scale tanks. Description of the various tank configurations and the details of the modeling techniques used are provided. Experimental observations made at the 2 L scale are presented and the rationale behind choosing the right scale up parameter is explained.

The later part illustrates development of the correlation by combining the experimental data with the fundamental hydrodynamic property obtained from the CFD simulation. This correlation is then extended to the commercial scale tanks based only on the CFD model. Validation of the developed correlation against the 10 L scale data is reported at the end.

The objective of the present study is to establish a combinatorial approach using CFD modeling and experimentation to establish a scale-up rule for scaling up liquid mixing applications that involve draw down of light weight solids. The user will be able to select operating conditions at large scale based on experimental observations at small scale and utilizing CFD model predictions.

2. Experimental methods

Four different tank configurations as shown in Fig. 2 were chosen for this study based on the existing tanks in the commercial scale facility. These non-standard configurations include two unbaffled geometries, two geometries with angled shafts and one geometry with off-centered shaft. Data related to nonstandard tank geometries is scarce in the literature hence generation of in-house data was necessary for proper scale up.

The experiments were performed at the lab scale 2L stirred tanks. The rationale for selecting the 2L scale for lab scale studies was to minimize the material utilization during scale down studies. Availability of material is often a limiting factor for scale down studies in the pharmaceutical industry. The experiments in the commercial scale tank are planned for the future. The 2L scale stirred tanks were designed to be geometrically simi-

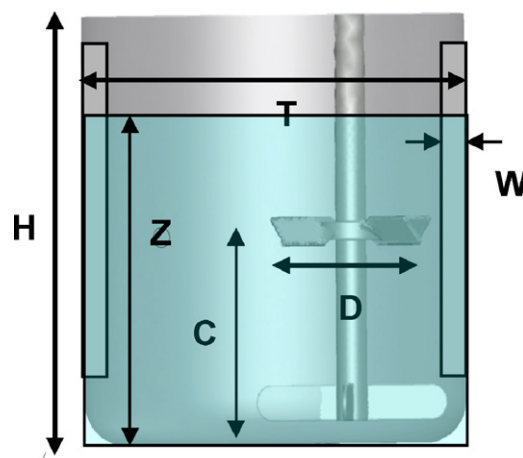


Fig. 3. Illustration of key tank dimensions.

lar to the four different large scale tanks. Key aspect ratios were maintained constant across both the scales. The key ratios are – impeller diameter/tank diameter (D/T), liquid height/tank diameter (Z/T), impeller clearance from the tank bottom/tank diameter (C/T), distance between the impellers/tank diameter, baffle width/tank diameter (W/T). Fig. 3 illustrates these key tank dimensions and Table 1 lists the absolute values of these ratios on both the scales for direct comparison.

It should be noted that although the key ratio of the impeller diameter/tank diameter was held constant but it was practically not

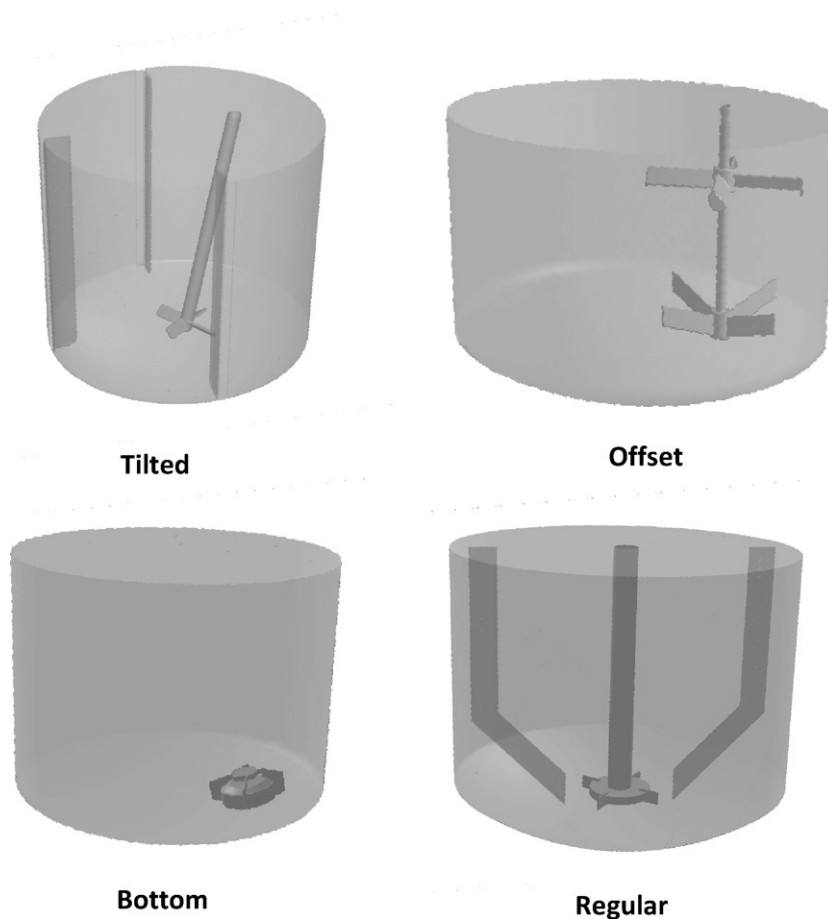


Fig. 2. Four different mixing tank configurations used in this study. Configurations are based on the existing tank geometries in the commercial scale facility. Note that bottom impeller configuration has no shaft because it uses magnetically coupled drive.

Table 1
Key tank dimension and aspect ratios at both the scales.

Tank	Impeller type	Baffles	T (cm)	Fill volume(L)	D/T	C/T	W/T	Z/T
Commercial								
Bottom	Non-standard up-pumping	0	39.6	40	0.25	0	0	0.85
Tilted ^a	45° PBTD	3	50.2	151	0.28	0.17	0.1	1.06
Offset ^b	45° PBTD ^c & paddle2	0	172.7	2500	0.41	0.02	0	0.65
Offset	45° PBTD & paddle	0	172.7	3600	0.41	0.02	0	0.93
Regular	4 bladed Rushton	2	41	42	0.26	0.11	0.08	0.87
Lab								
Bottom	Non-standard up-pumping	0	15.1	2.1	0.25	0	0	0.84
Tilted	45° PBTD	3	15.1	2.3	0.25	0.17	0.1	1.06
Offset	45° PBTD & paddle	0	15.1	1.58	0.42	0	0	0.64
Offset	45° PBTD & paddle	0	15.1	2.35	0.42	0	0	0.92
Regular	4 bladed Rushton	2	15.1	1.75	0.25	0.17	0.08	0.86
Validation								
Centered/baffled	45° PBTD	2	23.4	10	0.625	0.5	0.1	1
Centered/no baffle	45° PBTD	0	23.4	10	0.625	0.5	0.1	1
Tilted/baffled	45° PBTD	2	23.4	10	0.625	0.33	0.1	1
Tilted/no baffle	45° PBTD	0	23.4	10	0.625	0.33	0.1	1

^a Tilted impeller is placed at an angle of 15° with the vertical.

^b Both the impellers in the Offset configuration are of the same diameter.

^c PBTD – pitched blade turbine down-pumping availability.

possible to scale down the impeller blade thickness with the appropriate ratio. The small scale impeller has to be of a certain minimum thickness for enough mechanical strength. Hence, the resulting ratio of the impeller thickness/impeller diameter at the lab scale was higher than those at the commercial scale. Effect of different ratios of impeller thickness/impeller diameter at different scale is not completely understood although there have been attempts to study the effect of blade thickness at a single scale and same geometry. Chapple et al. (2002) reported that effect of blade thickness depends on the type of impeller. In case of Rushton turbines, the power number is sensitive to blade thickness but is independent of D/T ratio. On other hand, pitched blade turbines show sensitivity towards the D/T ratio but not towards blade thickness.

Although care was taken to maintain the exact geometric similarity across both the scales, the shape of the bottom of the 2 L tank was not identical to the commercial tanks. The 2 L tank is made up of a single glass vessel; hence it was not possible to match the shape of the bottom with each of the individual commercial tanks. The 2 L tank was designed in such a way that the regular and the tilted impeller tank configurations had the original hemispherical tank bottom. A flatter, dish like, false tank bottom was built for the offset and the bottom impeller tanks (see Fig. 4). It was anticipated that the different tank bottom shapes would not affect the mixing characteristics at the surface and hence should result into minimal influence on solids drawdown. The 2 L tank assembled in various configurations is shown in Fig. 4. The abovementioned slight differences between the lab and the commercial scale geometries were accurately captured during CFD simulation.

Additionally, an intermediate scale tank of volume 10 L (Fig. 5) was used for the validation of the correlation developed in this study. This tank had different geometric ratios than the previously studied tanks at the 2 L and the commercial scale (see Table 1). This makes the 10 L tank a good test case to assess the validity of the correlation upon change of scale as well as upon change of geometry. Four different tank configurations with variation in impeller angles (centered/tilted) and baffles (w and w/o) were investigated.

Deionized water at room temperature was used as a model liquid for all the experiments. Fumed silica (CABOSIL M5P manufactured by CABOT) was used as a model solid to study floating solids drawdown phenomenon. Fumed silica is a light, fluffy powder commonly used in pharmaceutical formulations to alter the viscosity of liquid formulations. Fumed silica has a solid density of 2.2 g/cc but the bulk density for uncompressed fumed silica is around 0.05 g/cc. Only one model compound was used in this study because the

effects of particle characteristics such as density, size, sticking tendency, wetting characteristics were outside the scope of the current work. Focus of this study was on the effects of tank geometry and scale on solids drawdown. The fumed silica was added manually from the top through a funnel. Rate of addition of the silica (g/min) was maintained constant within human error. Solids slowly start accumulating on the liquid surface if the rate of continuous addition exceeds the maximum drawdown rate. The fumed silica was added at different rates and the maximum rate at which no solids build up was observed was identified visually. This rate was designated as the drawdown rate from the free liquid surface. Stirrer speed was varied from 50 to 800 rpm and drawdown rate was measured as a function of the stirred speed for the various tanks. Solids loading was maintained below 1 wt% through out the experiments to minimize the changes in the liquid physical properties. A few selected experimental conditions were repeated in triplicates to gain an estimate of the experimental variability.

3. Computational methods

CFD fluid flow simulations were performed for all the four tank configurations at both the 2 L and the large scale. Tank geometries were generated and meshed using Gambit 2.4.6 meshing software. Each tank was meshed using size function such that the cell size increased with smallest cells near the impeller blade and largest cells near the wall. Fig. 6 shows one representative mesh created for commercial scale offset impeller configuration. Number of cells for each tank varied from approximately 300,000 to 800,000. A grid independence study was not performed for this work but it is a standard practice to use few hundred thousand grid elements to model industrial scale tanks (Ranade, 2002).

The CFD simulations were performed using a commercial software package Fluent 6.3.26. All the cases were modeled as single phase, steady state with multiple reference frame (MRF) formulation. More accurate unsteady state sliding mesh model was not chosen for this work because it needs more computational resources. The sliding mesh formulation may take up to a week to converge as compared to 1–2 days needed for the MRF formulation. Additional computational burden of the sliding mesh simulations for 8 tanks was prohibitive. RNG $k-\varepsilon$ turbulence model was used for all the cases. It has been shown that RANS-based CFD simulations of stirred tanks using two-equation turbulence models such as the RNG $k-\varepsilon$ model can under-predict quantities such as turbulence kinetic energy and dissipation rate (Yeoh et al., 2004).

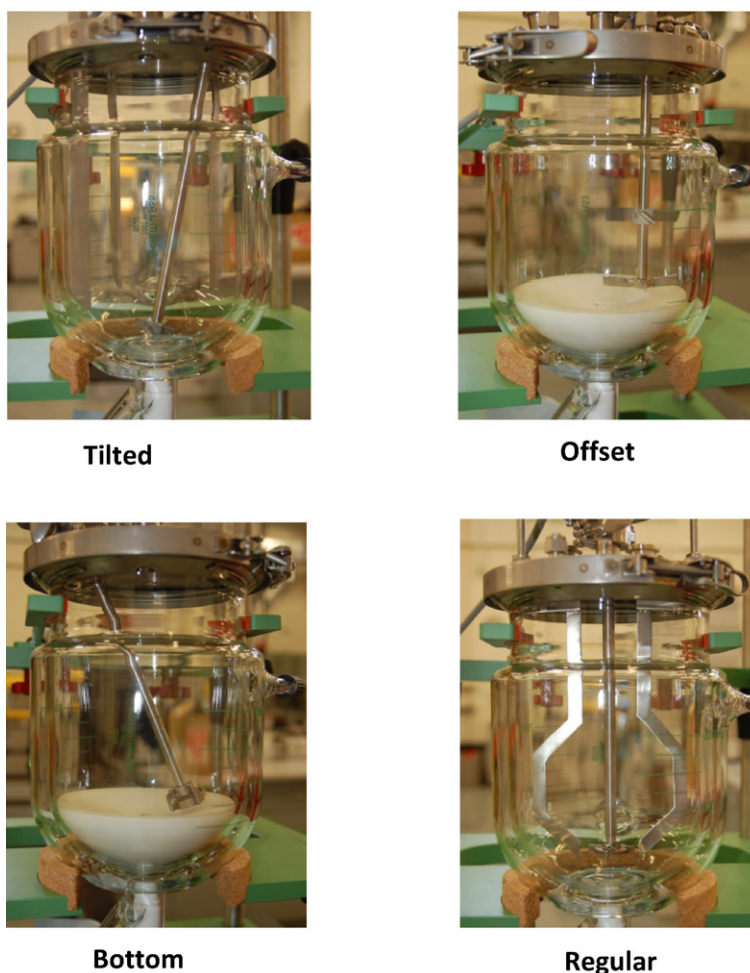


Fig. 4. Photographs of the fabricated 2L scale stirred tank configurations.

However, it has also been shown that these types of simulations can predict flow quantities such as mean fluid velocity with reasonable accuracy (Harris, 1996). It was assumed that the distortion of the free liquid surface is negligible hence free surface was treated as symmetry boundary condition. No slip wall boundary condition was used for tank wall, impeller, shaft and baffles. Simulations were run until the force on the impeller and the flow rate through the impeller reached a steady state. It was made sure that the residuals were below 10^{-3} at the end of the simulations.

Discrete phase modeling (DPM) available in Fluent was used to model the movement of inert solid particles to simulate drawdown of floating solids. The DPM models perform Lagrangian tracking of particles assuming only one way coupling between liquid and solid. In order to perform DPM simulations, first a converged flow field solution was obtained and then the flow equations were turned off during the DPM simulations. The density of the solids at the instant when it is pulled into the liquid is neither the bulk density of the solid (0.05 g/cc) nor the true density (2.2 g/cc). In reality when the solids come in contact with the liquid surface, wetting of solid phase occurs resulting into a density somewhere in between those two extremes. It is rather difficult to quantify the extent of wetting and hence obtain the exact density of solids when it gets pulled into the liquid. Due to the lack of this information density of 0.92 g/cc was assumed for the CFD simulation such that it is greater than the true density of solids and lower than the bulk density.

Particles of diameter 0.1 mm were injected uniformly from the top liquid surface. The goal was to calculate residence time of particles on the top liquid surface. It was not possible to sample particles

at the same plane as the injection plane because in that case the residence time would have been zero. Hence, for simulation purposes, the surface of the liquid was assumed to be a thin layer of liquid at the top of the tank. The thickness of this thin layer was chosen to be as small as possible without adversely affecting the quality of the grid. The thickness was fixed at 5 mm for all the geometries and a sampling plane was created 5 mm below the top liquid surface (see Fig. 7). This arbitrary choice of 5 mm thickness would not affect residence time in the same proportion for all tanks. Particles were trapped once they hit the sampling surface to avoid double counting. Average time taken by the particles to reach the sampling plane was calculated. This time was designated as the residence time of the particles on the surface. Inverse of the residence time is a measure of the drawdown rate of particles.

4. Results and discussions

4.1. Experimental

Results of the lab scale experiments conducted in the 2L tank are shown in Fig. 8. The experimentally measured drawdown rates are plotted as a function of the stirrer speed for the various tank configurations. For a given tank geometry the drawdown rate was linearly proportional to the stirrer speed. Linear regression showed a good linear fit with coefficient of correlation ranging from 0.99 to 0.97 for various tank geometries. A wide spread in the drawdown rate at a constant rpm can be seen for the different tank configura-

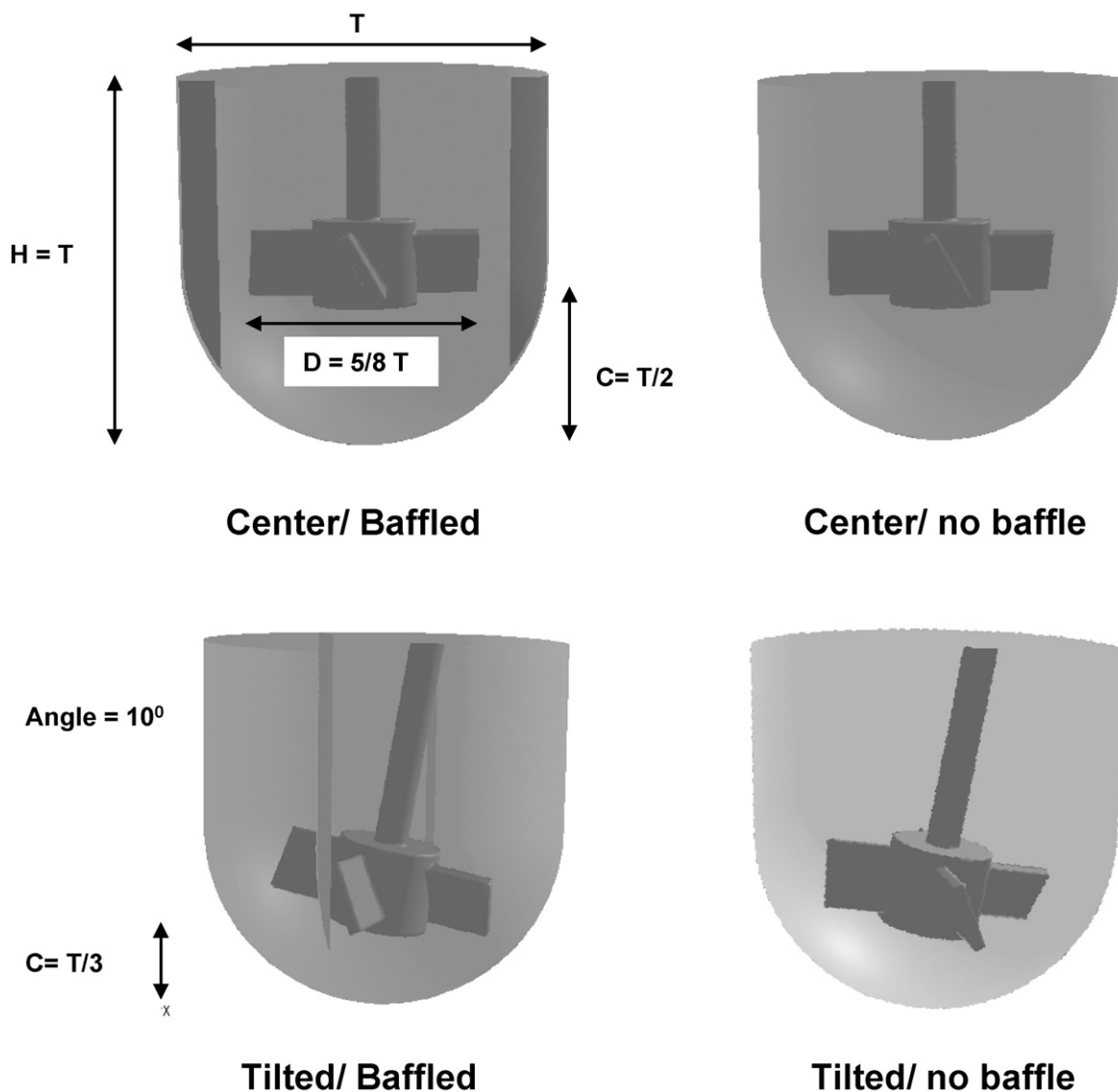


Fig. 5. Illustration of the four different tank geometries studied at the 10L scale.

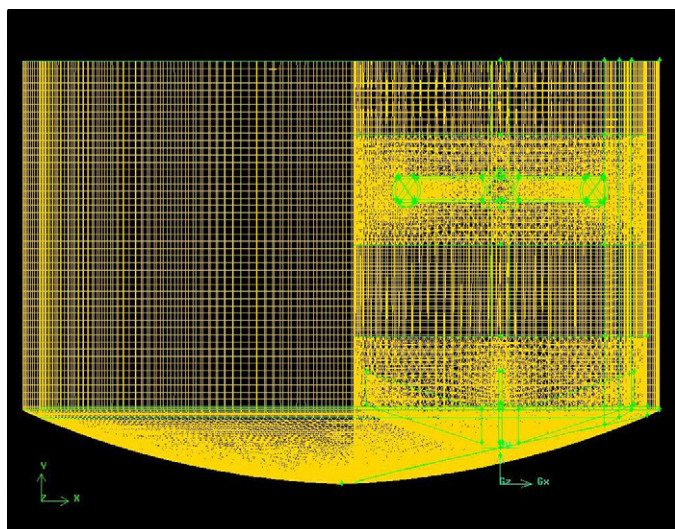


Fig. 6. Mesh for commercial scale offset impeller configuration created using commercial meshing software GAMBIT2.4.6.

tions. The offset impeller tank showed maximum drawdown rate owing to the fact that it has two impellers and the top impeller is closer to the liquid surface.

4.2. CFD model

Fig. 9 shows CFD simulation results in the form of the contours of the velocity magnitude for the different mixing tank configurations. The rationale for keeping the geometric similarity between both the scales is to ensure a similar flow patterns across both the scales. Fig. 10 shows representative velocity vectors for the tilted impeller configuration at similar P/V value. The P/V values were obtained from the CFD simulation using the torque acting on the impeller (Paul et al., 2004). The velocity vectors confirm that the flow pattern is indeed similar across both the scales. This is an important validation step in the scale up procedure.

4.3. Combining experimental results with CFD for 2L scale

As a first step towards developing a correlation for solid drawdown rate it is important to identify a governing mechanism for the drawdown of particles. As discussed in Section 1, there are

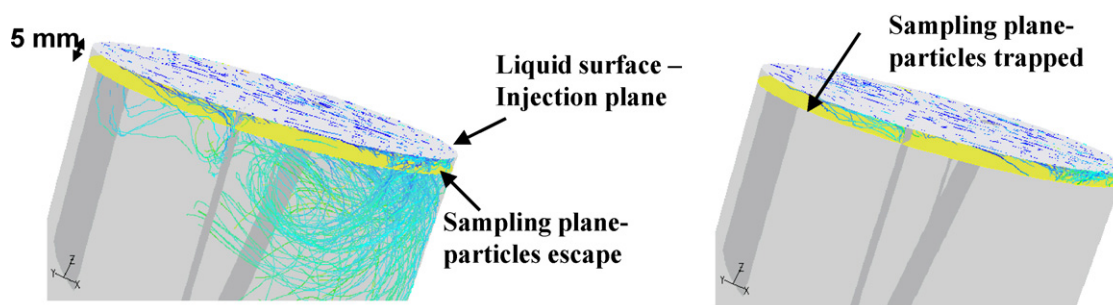


Fig. 7. Schematics of the DPM model set up.

three mechanisms responsible for drawdown (Khazam and Kresta, 2008). Relative importance of these mechanisms for the current set of experimental conditions can be assessed as follows:

- (1) Stable vortex formation – none of the geometries studied at the 2 L scale show strong vortex formation at the surface. The two geometries without the baffle use either an impeller placed at an angle (bottom impeller) or placed off-centered (offset impeller). This arrangement helps in breaking symmetry and prevents strong vortex formation. Moderate vortex formation was observed experimentally for the offset impeller configuration. The tilted impeller geometry consists of three baffles which are enough for preventing vortex formation. The regular impeller geometry where impeller is placed vertical at the center was equipped with two baffles and did not show strong vortex formation for the stirrer speeds investigated. Based on the visual observation it was concluded that stable vortex formation is not the major mechanism of the drawdown but it might contribute in the offset impeller configuration.
- (2) Turbulent fluctuations – Khazam and Kresta (2008) found this mechanism to be dominant for the cases where low submergence was used. For present study, only offset impeller geometry with two impellers had an impeller close to the liquid surface. This mechanism might contribute to a certain extent in that case.
- (3) Mean drag – examination of velocity field obtained from CFD simulation showed strong axial velocity components for all the tank geometries under investigation. Hence it was assumed that the mean drag is the most significant mechanism of solid drawdown for all the cases under consideration.

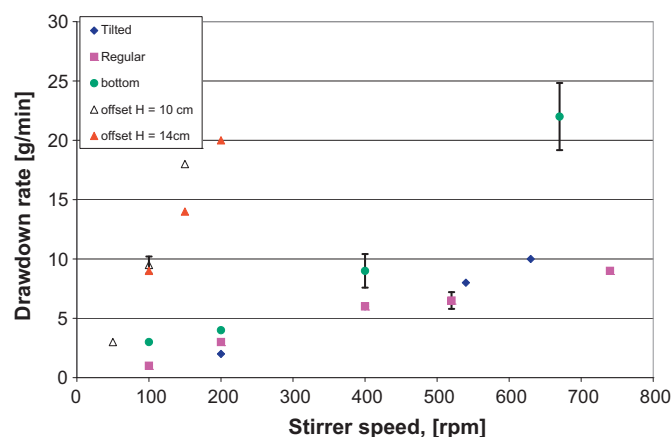


Fig. 8. Experimentally measured maximum fumed silica drawdown rate as a function of stirrer rpm for the different lab scale tanks.

The drawdown mechanism for each type of the tank geometry is also tabulated in Table 2.

Mean drag acting on a single solid particle is a function of slip velocity between the solid phase and the liquid phase. The slip velocity in turn depends on the mean velocity of the liquid phase. Based on this understanding it was deduced that the particle drawdown rate should be governed by the velocity at the free liquid surface. Velocity is a vector and varies across the entire liquid surface. To simplify the analysis, it was assumed that the overall strength of the velocity field is represented by the velocity magnitude averaged over the entire liquid surface. This quantity will be referred as the average surface velocity. CFD simulations were performed to obtain the velocity field for various tanks as shown in Fig. 9 and Fig. 10.

Fig. 11 shows the experimentally measured drawdown rates for the 2 L tank plotted against the average surface velocity. The average surface velocity was obtained from the CFD simulation results. It can be seen that the drawdown rate correlates linearly with the average surface velocity and the relationship is independent of the mixing tank configuration. Different tank configurations show similar drawdown rates at similar average surface velocities. It should be noted that the same average surface velocity can be obtained at different stirrer speeds for different tank configurations. Using fundamental hydrodynamic property (velocity) results in subtraction of the effect of geometry from the tank performance.

4.4. Extension to large scale tanks

Fig. 11 suggests that the drawdown rate can be correlated to the average surface velocity for the 2 L scale mixing tanks but it is not clear how the change in scale will affect the drawdown rate. Practically it was not possible to perform experiments on the commercial scale equipment to discern the effect of scale hence drawdown of particles was simulated using models. CFD simulations in conjunction with Lagrangian particle tracking (DPM) were utilized to model the movement of inert solid particles. Residence time of particles on the liquid surface was calculated as explained in Section 3. Drawdown rate is inversely proportional to the residence time.

Fig. 12 shows the particle tracks obtained from the DPM simulation. A careful examination of the particle tracks reveals two different mechanisms for the solid drawdown. According to the first mechanism, particles tend to travel towards the tank wall

Table 2
Primary mechanism of drawdown for each tank configuration.

Tank Configuration	Primary mechanism of drawdown
Tilted	Mean drag
Offset	Mean drag assisted by stable vortex formation and turbulent fluctuations
Bottom	Mean drag
Regular	Mean drag

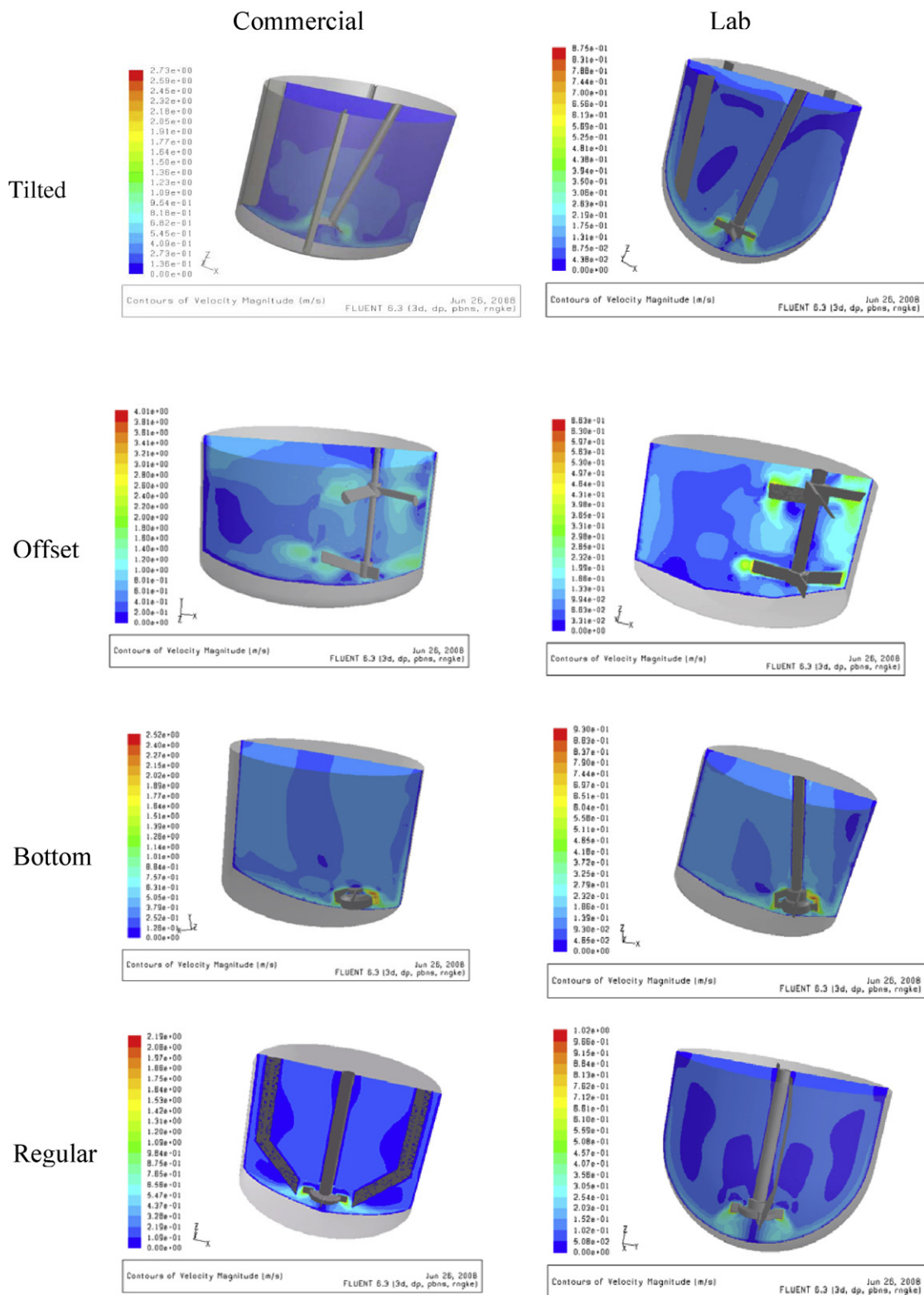
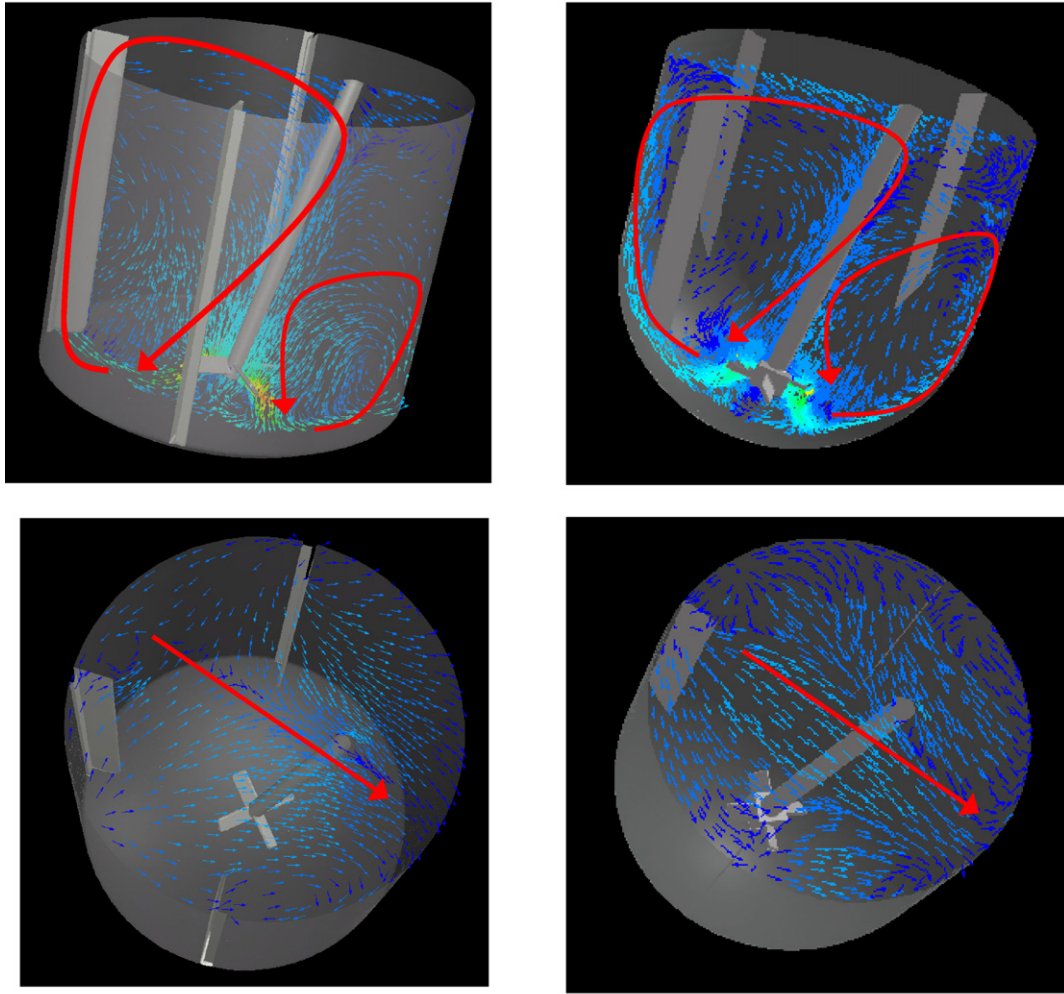


Fig. 9. Contours of velocity magnitude obtained from the CFD simulations.

before getting pulled into the liquid due to the downward velocities near the wall. This mechanism was found to be the dominating mechanism for all the tanks except the offset impeller configuration. In the offset impeller configuration, the second mechanism was found to be dominant where particles follow a circular path and then get pulled down through a vortex. This observation sug-

gests that the previous assumption of mean drag being the most important mechanism of drawdown may not be valid for the offset impeller tank. This will be shown later in the validation section that the correlation fails to accurately predict drawdown rate for the cases with strong vortex formation because of the breakdown of this assumption.



Tilted impeller : Commercial scale
RPM = 250, P/V = 40 W/m³

Tilted Impeller: Lab scale
RPM = 540, P/V = 45 W/m³

Fig. 10. Velocity vector plot for the tilted impeller geometry showing the similarity between the flow patterns across both the scales.

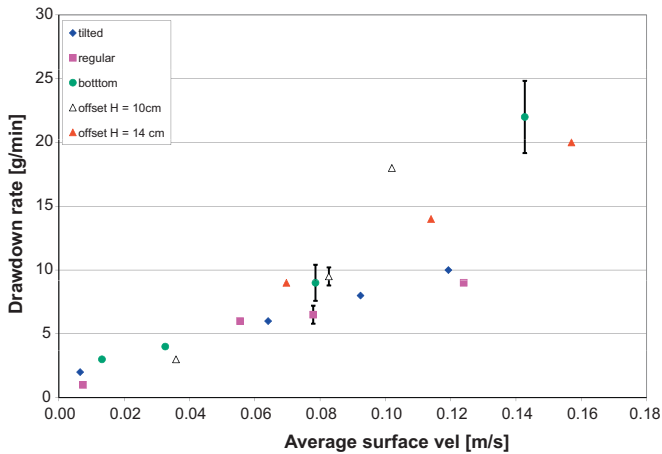


Fig. 11. Graph showing the linear relationship between the experimentally measured drawdown rates as a function of the average surface velocity obtained from CFD modeling.

Understanding the mechanism of the solids drawdown suggests that the particle residence time on the surface should be linearly proportional to the tank diameter. In case of larger tanks, the particle has to travel greater distance to reach the wall before getting pulled into the liquid resulting in higher residence time. On the other hand, residence time would be shorter if the surface velocity is higher. Overall, it can be claimed that.

$$\frac{1}{\text{residence time}} \propto \frac{\text{average surface velocity}}{\text{tank diameter}} \quad (2)$$

The average surface velocity/tank diameter can be used as a scale-up parameter. It means that 1/residence time should be equal at constant average surface velocity/tank diameter, irrespective of the scale or the tank configuration. Fig. 13 verifies this hypothesis where the 1/residence time obtained from the DPM simulations was plotted against the surface velocity/tank diameter. Data for both the lab scale and the commercial scale tanks followed a single line with some variation as seen in Fig. 13. The 1/residence time values for the commercial scale tank appear to be systematically slightly higher than the lab scale data. The exact reason for this

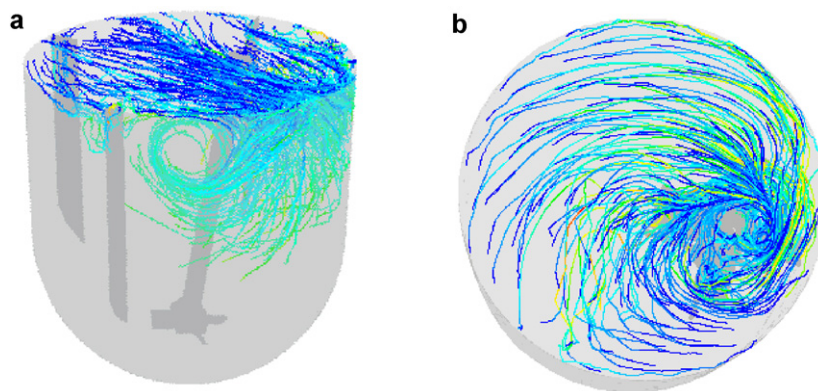


Fig. 12. Particle tracks showing two distinct drawdown mechanisms. (a) Drawdown along the wall for the 2 L tilted impeller geometry at 540 rpm. (b) Drawdown through a vortex for the 2 L offset impeller geometry at 150 rpm, liquid height = 10 cm.

systematic difference is not very clear at this point and deserves additional study at the large scale.

4.5. Final correlation

The DPM simulations proved that the 1/residence time is proportional to the average surface velocity/tank diameter. In reality, the absolute value of the drawdown rate is solid phase specific. Drawdown rate depends on the solids properties such as particle diameter, density, particle–liquid interaction (wettability) and particle–particle interactions (stickiness). To take this effect into account, the final correlation for the drawdown rate was based on the actual experimental data rather than the DPM simulations. Fig. 14 shows the experimentally measured drawdown rate plotted against the average surface velocity/tank diameter obtained from CFD simulations. The drawdown rate for the commercial scale tanks can be predicted based on linear fit to this data. A correction factor needs to be included in this formula which will account for the fact that a higher surface area is available at the commercial scale for the drawdown of solids as compared to the smaller lab scale tanks. In other words it was hypothesized that the flux of the drawdown is proportional to the average surface velocity/tank diameter. Hence the final correlation for the drawdown rate at the commercial scale can be written as

$$\text{drawdown rate}_{\text{com}} = 17.25 \times \left(\frac{\text{surface velocity}}{\text{tank dia}} \right) \times \left(\frac{\text{tank area}_{\text{com}}}{\text{tank area}_{\text{lab}}} \right) \quad (3)$$

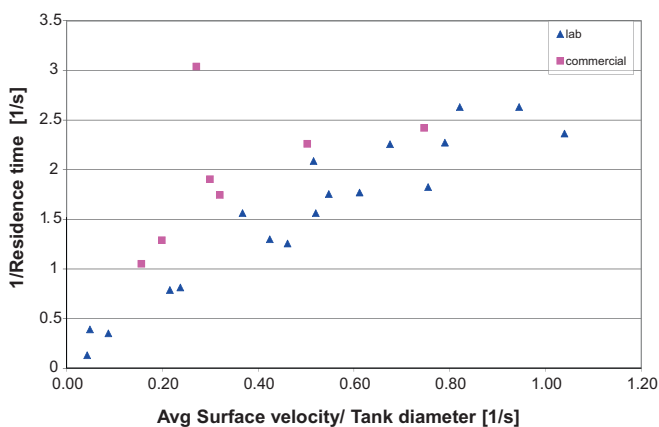


Fig. 13. Graph illustrating the linear relationship between 1/residence time vs. average surface velocity/tank diameter for the lab scale and the commercial scale mixing tanks. Both x and y axis quantities were obtained from the CFD simulations.

This correlation can be generalized as:

$$\text{drawdown rate}_{\text{com}} = k \times \left(\frac{\text{surface velocity}}{\text{tank dia}} \right) \times \left(\frac{\text{tank area}_{\text{com}}}{\text{tank area}_{\text{lab}}} \right) \quad (4)$$

where, constant k is a solid phase specific constant which can be obtained from experiments.

4.6. Model validation

Model validation was performed at the 10 L scale. The goal was to examine predictability of the correlation at a different scale as well as for a completely different geometry. Results of the solids drawdown experiments are shown in Fig. 15 in the form of parity plot for both baffled and unbaffled tank configurations. It can be seen from Fig. 15 that the correlation satisfactorily predicted the drawdown rate for both the baffled tank configurations, with the tilted impeller and with the straight impeller. Fig. 15 also shows the correlation over predicted the drawdown rate for the unbaffled tank configuration. Strong vortex flow observed in the unbaffled tanks might be the cause for the deviation from the correlation predictions. The correlation is based on the assumption that the mean drag is the only dominating mechanism of solids drawdown and it ignores the contributions from other mechanisms such as the turbulent engulfment and the stable vortex. The poor performance of the unbaffled tank as compared to the model prediction is in agreement with investigation by Khazam and Kresta (2008) who found that baffled tanks exhibit better drawdown rates as compared to

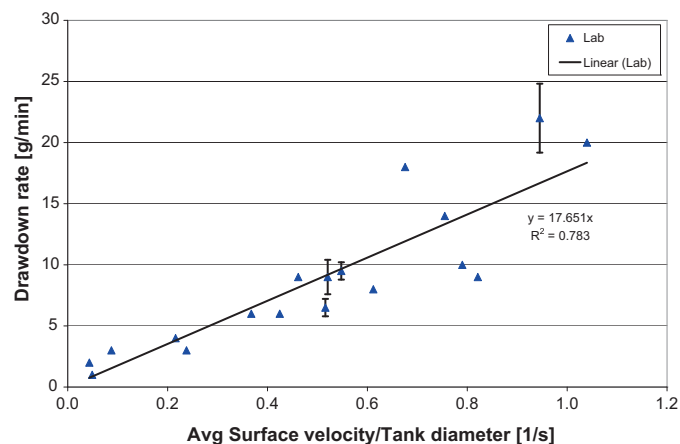


Fig. 14. Plot of the experimentally measured fumed silica drawdown rate against the average surface velocity/tank diameter.

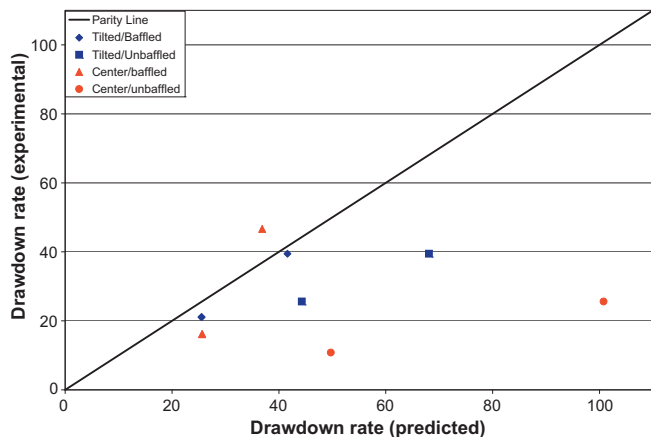


Fig. 15. Comparison of the predicted drawdown rate vs the experimentally measured drawdown rate for the 10 L baffled and unbaffled tank.

vortexing unbaffled tanks. Based on the results of the model validation experiments it is recommended that the correlation should be used for baffled, no vortex or mild vortex flows. This correlation should not be used with strongly vortexing flows or when the free surface is distorted. In future, a more accurate model can be developed using Multiphase CFD simulation which will accurately capture vortex and the surface distortions. Multiphase model might be able to provide a robust correlation that will work even for unbaffled tanks and vortexing flows. Experiments needs to be performed on commercial scale (40 L to 4000 L) to check the validity of model at that scale.

5. Conclusions

Experimental measurements of drawdown rate at the 2 L scale showed strong dependence of drawdown rate on the tank geometry and the stirrer speed. Mean drag was assumed to be the main mechanism of drawdown. Based on the CFD and DPM simulation at the 2 L and the commercial scale, it was postulated that the drawdown rate is proportional to the average surface velocity/tank diameter. A correlation was developed (Eq. (4)) where the proportionality constant k is solid phase specific and was found to be 17.5 for the fumed silica-water system under investigation. Model validation experiments conducted using a 10 L tank showed that the correlation predictions for drawdown rates were reasonably accurate for the case of low to mild vortexing flows. The correlation tends to over-predict the drawdown rate for strongly vortexing flows.

Acknowledgements

Authors would like to thank Fred Carroll, Brian Braxton and William Petre from Pfizer for valuable technical discussions.

References

- Bakker, A., Van den Akker, H.E.A., 1994. Single phase flow in stirred reactors. *Chem. Eng. Res. Des.* 72, 583–593.
- Bakker, A., Frijlink, J.J., 1989. The drawdown and dispersion of floating solids in aerated and unaerated stirred vessels. *Ind. Eng. Chem. Res.* 67, 208–210.
- Chapple, D., Kresta, S.M., Wall, A., Afacan, A., 2002. The effect of impeller and geometry on power number for a pitched blade turbine. *Chem. Eng. Res. Design.* 80, 364–372.
- Derksen, J.J., 2003. Numerical simulation of solids suspension in a stirred tank. *AIChE J.* 49, 2700–2714.
- Edwards, M.F., Ellis, D.I., 1984. The drawdown of floating solids into mechanically agitated vessels. *Inst. Chem. Eng. Symp. Ser.* 89, 1–13.
- Ellis, D.I., Godfrey, J.C., Majidian, N., 1988. A study of the influence of impeller speed on the mixing of floating solids in a liquid. *Fluid Mixing III* 181 (September), 8–10.
- Harris, C., 1996. Computational fluid dynamics for chemical reactor engineering. *Chem. Eng. Sci.* 51, 1569–1594.
- Hemrajani, R.R., Smith, D.L., Koros, R.M., Tarmy, B.L., 1988. Suspending floating solids in stirred tanks – mixer design, scale-up and optimization. In: *Proc. Sixth European Conference on Mixing*, Milan, Italy, pp. 259–265.
- Joosten, G.E.H., Schilder, J.G.M., Broere, A.M., 1977. The suspension of floating solids in stirred vessels. *Trans. Inst. Chem. Eng.* 55, 220–222.
- Kerdouss, F., Bannari, A., Proulx, P., Bannari, R., Skrga, M., Labrecque, Y., 2008. Two-phase mass transfer coefficient prediction in stirred vessel with a CFD model. *Comp. Chem. Eng.* 32, 1943–1955.
- Khazam, O., Kresta, S.M., 2008. Mechanisms of solids drawdown in stirred tanks. *Can. J. Chem. Eng.* 86, 622–634.
- Khazam, O., Kresta, S.M., 2009. A novel geometry for solids drawdown in stirred tanks. *Chem. Eng. Res. Des.* 87, 280–290.
- Khopkar, A.R., Rammohan, A.R., Ranade, V.V., Dudukovic, M.P., 2005. Gas–liquid flow generated by a Rushton turbine in stirred vessel: CARPT/CT measurements and CFD simulations. *Chem. Eng. Sci.* 60, 2215–2229.
- Kresta, S.M., Wood, P.E., 1991. Prediction of three dimensional turbulent flow in stirred tanks. *AIChE J.* 1, 448–460.
- Kuzmanic, N., Ljubic, C., 2001. Suspension of floating solids with up-pumping pitched blade impellers; mixing time and power characteristics. *Chem. Eng. J.* 84, 325–333.
- Ljungqvist, M., Rasmuson, A., 2001. Numerical simulation of the two-phase flow in an axially stirred vessel. *Chem. Eng. Res. Des.* 79, 533–546.
- Micale, G., Grisafi, F., Rizzuti, L., Brucato, A., 2004. CFD simulation of particle suspension height in stirred vessels. *Chem. Eng. Res. Des.* 82, 1204–1213.
- Montante, G., Micale, G., Magelli, F., Brucato, A., 2001. Experiments and CFD predictions of solid particle distribution in a vessel agitated with four pitched blade turbines. *Chem. Eng. Res. Des.* 79, 1005–1010.
- Murthy, B.N., Ghadge, R.S., Joshi, J.B., 2007. CFD simulation of gas–liquid–solid stirred reactor: prediction of critical impeller speed for solid suspension. *Chem. Eng. Sci.* 62, 7184–7195.
- Ozcan-Taskin, G., McGrath, G., 2001. Draw down of light particles in stirred tanks. *Chem. Eng. Res. Des.* 79, 789–794.
- Özcan-Taşkin, G., Wei, H., 2003. The effect of impeller-to-tank diameter ratio on draw down of solids. *Chem. Eng. Sci.* 58, 2011–2022.
- Özcan-Taskin, G., 2006. Effect of scale on the draw down of floating solids. *Chem. Eng. Sci.* 61, 2871–2879.
- Paul, E.L., Atiemo-Obeng, V., Kresta, S.M., 2004. *Handbook of Industrial Mixing*, First ed. John Wiley & Sons, New Jersey.
- Ranade, V.V., 2002. *Computational Flow Modeling for Chemical Reactor Engineering*, First ed. Academic Press, San Diego.
- Sahu, A.K., Kumar, P., Patwardhan, A.W., Joshi, J.B., 1999. CFD modeling and mixing in stirred tanks. *Chem. Eng. Sci.* 54, 2285–2293.
- Siddiqui, H., 1993. Mixing technology for buoyant solids in a nonstandard vessel. *AIChE J.* 39, 505–509.
- Srinivasa, T., Jayanti, S., 2007. An Eulerian/Lagrangian study of solid suspension in stirred tanks. *AIChE J.* 53, 2461–2469.
- Yeoh, S.L., Papadakis, G., Yianneskis, M., 2004. Numerical simulation of turbulent flow characteristics in a stirred vessel using the LES and RANS approaches with the sliding/deforming mesh methodology. *Chem. Eng. Res. Des.* 82, 834–848.